Pharmaceutical Research, Vol. 26, No. 12, December 2009 (© 2009)
DOI: 10.1007/s11095-009-9979-y

Research Paper

The Influence of Flow Rate on the Aerosol Deposition Profile and Electrostatic Charge of Single and Combination Metered Dose Inhalers

Susan Hoe,[1] Daniela Traini,[1] Hak-Kim Chan,[1] and Paul M. Young[1,2]

Received August 11, 2009; accepted September 14, 2009; published online October 6, 2009

Purpose. The capability of the electrostatic next generation impactor (eNGI) has been investigated as a tool capable of measuring the electrostatic charge of single (Flixotide™; containing fluticasone propionate (FP)) and combination (Seretide™; FP and salmeterol xinafoate (SX)) pressurised metered dose inhalers (pMDIs) at different flow rates.
Methods. Aerosol mass distributions were investigated at 30, 60 and 90 $l.min^{-1}$ and simultaneous charge measurements recorded.
Results. Analysis of the mass distribution data indicated a flow dependent relationship, where the aerosol performance (aerodynamic diameter <5 μm) of FP significantly increased between 30 $l.min^{-1}$ and 60 $l.min^{-1}$ for both formulations. No significant increase in SX was observed for Seretide with increased flow rate. Analysis of the charge distribution indicated both formulations to primarily charge negatively with a concurrent increase in charge with increased flow rate. Interestingly, the charge-tomass ratio remained relatively constant between 30 $l.min^{-1}$ and 60 $l.min^{-1}$ and increased at 90 $l.min^{-1}$, indicating that charging was majorly influenced at the highest flow rate.
Conclusions. This study has shown how the eNGI could be used as a simple Pharmacopeia based methodology for the evaluation of mass and charge profiles of single and combination pMDIs at a series of flow rates.

KEY WORDS: electrostatic NGI; electrostatics; eNGI pMDI; flow rate; inhalation.

INTRODUCTION

Pressurised metered dose inhalers (pMDIs) are pocket sized, respiratory medicines for the treatment of asthma and other respiratory related diseases. They contain a drug, either suspended or solubilised, in a hydro-fluoro-alkane (HFA) propellant with or without co-solvents or stabilising excipients. Upon actuation, the pressurised liquid HFA is exposed to atmospheric pressure and rapidly expands to its gaseous state. This rapid phase transition is utilised to aerosolise the medicament as small particles or droplets for inhalation. The respiratory deposition and therapeutic efficiency of pMDI devices is dependent on a number of factors including: particle size (generally accepted as <6 μm (1)), plume exit velocity and geometry as well as inhalation (inspiratory) flow rate and the electrostatic charge of the aerosol particles.

The patient's inspiratory flow rate, during actuation of a pMDI, will have direct influence on lung deposition due to the respiratory architecture (2). However, variation in the inspiratory flow rate may also alter the intrinsic properties of the aerosol ex-valve, affecting the particle size and charge distribution. The British/European Pharmacopeia (BP, Ph. Eur) and United states Pharmacopeia (USP) method(s) for assessing aerosol size distribution are cascade impactors (3,4). These include the multi-stage liquid impinger (MSLI), the Anderson cascade impactor (ACI), the Marple Miller impactor (USP only (3)) and the next generation impactor (NGI). These impactor methodologies measure the mass distributions of particles as a function of aerodynamic diameter, and generally report the fine particle mass (FPM) (or fraction (FPF)) of particles with a diameter <5 μm as being suitable for respiratory delivery. Furthermore, by altering the internal impactor architecture, or interpolating a mass-size distribution profile, it becomes possible to calculate the FPM or FPF at variable flow rates.

Previous studies of the effect of inspiratory flow rate on pMDI performance have produced conflicting results. A study by Ross and Shultz (5) showed no variability in the FPM (<5 μm) between 30 and 60 $l.min^{-1}$ flow rates, when studying the performance of five commercial pMDI products using the Marple Miller impactor: Ventolin™ (90 μg salbutamol sulphate (SS), Allen & Hanburys); Beclovent™ (42 μg beclomethasone dipropionate (BDP), Allen & Hanburys); Pulmicort™ (200 μg budesonide (BUD), Astra); and Brethaire™ (200 μg Terbutaline sulphate, Geigy). However, it is important to note that in this study the findings are questionable, since the error associated with the emitted dose and FPM were high (relative standard deviations for the pMDI FPM ranged from 4% to 22%). In comparison Terzano and Mannino (6) found variations in particle size with flow rate when studying pMDI formulations

[1] Advanced Drug Delivery Group, Faculty of Pharmacy, University of Sydney, Sydney, NSW 2006, Australia.
[2] To whom correspondence should be addressed. (e-mail: py@pharm.usyd.edu.au)

containing fluticasone propionate (FP), flunisolide or BDP. In general, this study showed a decrease in the percentage of particles <5 μm with increased flow rate (when comparing 30 l.min^{-1} to 60 l.min^{-1}). It is important to highlight that this study did not utilise conventional impactor methodology, instead opting for a time-of-flight laser diffraction technique (Aerosizer™ with AeroBreather®: API Inc, Hadley, MA, USA) (7). Time-of-flight measurement is significantly different to conventional impaction techniques (7,8) and the differences observed may be due to a multitude of factors including: mass deposition in the AeroBreather®, sample dilution, aerosol analysis flow rate (typically <2.5 l.min^{-1})(8) and a lack of drug mass determination.

In comparison, Smith *et al.* (1999) observed a significant increase in the FPF (< 5 μm) of Respolin™ (100 μg SS (3 M)) FPF when the flow rate was increased from 30 l.min^{-1} to 55 l.min^{-1} using a Marple Miller impactor (9). Similarly, a later study by Feddah *et al.* (10) showed significant increases in FPF (<5 μm) for Flixotide™, (250 μg FP), Pulmicort™ (200 μg BUD) and Becotide™ (100 μg BDP), all Allen & Hanburys, when the operating flow rate of a Marple Miller impactor was increased from 30 l.min^{-1} to 60 l.min^{-1}. Furthermore, both these studies investigated the performance of these systems at higher flow rates (80–90 l.min^{-1}). However, the reported change in FPM or FPF are difficult to compare, since the upper cut-off size limit for calculating FPF/FPM varied at the higher flow rate, and as such those FPF/FPM results cannot be compared.

Interestingly, there is no Pharmacopoeia method for studying aerosol charge, even though its presence in aerosol medicines has been suggested to affect formulation performance and lung deposition. For example, previous computational (11–13), *in vitro* (14,15) and *in vivo* (16) studies have suggested that charged aerosol particles may effect deposition in the throat and respiratory system. Furthermore, the charge generated during the aerosolisation of pMDI formulations, when using spacer devices, has been shown to potentially reduce the therapeutic dose, via particle wall interaction (17–20). Subsequently, the industry has developed stringent cleaning and maintenance instructions to avoid static charge in many spacer devices.

Up to now, the state-of-the art for measuring aerosol electrostatic charge as a function of aerodynamic particle diameter (and mass distribution) has been the electrical low pressure impactor (ELPI) (21). Although not a pharmacopoeia methodology, the ELPI is based on a low-pressure impactor, where each stage is electrically isolated and the charge associated with particles as they impact can be measured via an electrometer. While primarily designed for the measurement of atmospheric, combustion, and work place aerosols, the application of the ELPI for measuring the charge in pMDI formulations has received some interest. Glover and Chan studied the potential of the ELPI for measuring the mass deposition and electrostatic charge of Ventolin™ (100 μg SS) and Flixotide™ (250 ug FP) (22). In this initial study, the authors showed variations in charging profile between pMDI formulations and reported the operating conditions for successful measurement. In a later study, Kwok *et al.*, studied five commercially available pMDI formulations using the ELPI (Ventolin™ (100 μg SS), Flixotide™ (250 μg FP), QVAR™ (100 μg BDP), Intal Forte™ (5 mg disodium cromoglycate; Aventis Pharma) and Tilade™ (2 mg nedocromil sodium; Aventis Pharma)) (23). In this study, Kwok *et al.*, discussed the influence in formulation and device components on the charge profile (for example mono and bipolar charging characteristics), and reported time dependent effects for Ventolin™ and QVAR™ formulations. Another study by the same group focussed on using the ELPI to evaluate pMDI charge and mass profiles with add-on spacer devices and reported the charge associated with the internal spacer lining had a significant negative impact on the resulting FPF and aerosol charge profiles (17). For further information regarding the electrostatic phenomena in pMDI systems and related studies within the field, the authors refer the reader to the excellent review by Mitchell *et al.*, (19). Although the ELPI is a useful tool to simultaneously study charge and aerosol mass deposition it has some limitations. For instance, the methodology is not based on a pharmacopeia recognised impactor architecture (3,4); the majority of the deposition stages are reported in the sub-micron region (24,25) and the sampling port flow rate operates at 10 or 30 l.min^{-1} (25).

The electrical-single particle aerodynamic relaxation time (E-SPART) analyser has been used to study charge distribution relative to particle size, on a particle-to-particle basis, enabling a higher resolution in determination of bipolar charging of aerosols (15,26–28). However, issues may arise with the characterisation of multi-component MDI and DPI formulations, where some components have similar particle size (such as drug and fines). As with the ELPI, the E-SPART is also not a recognised pharmacopoeia method.

The Next Generation impactor (NGI) is the most recently developed impactor, and was designed specifically for pharmaceutical aerosols (29,30). Recognised in pharmacopoeia as Apparatus E (Ph.Eur; (4)) or Apparatus 5 & 6 (USP; (3)) the NGI was designed to measure pharmaceutical relevant size distributions, operating between 30 and 100 l.min^{-1}. It includes a USP type throat and optional pre-separator for carrier based formulations. Recently, Hoe *et al.*, have adapted this impactor architecture to incorporate simultaneous charge measurement (31). Using the electrostatic next generation impactor (eNGI), Hoe *et al.*, demonstrated the eNGI capable of measuring the aerodynamic mass and charge distribution of three commercial pMDIs (Ventolin™ (100 μg SS), QVAR™ (100 μg BDP) and Flixotide™ (250 μg FP)) and directly compared the results to those obtained using an ELPI at an equivalent flow rate (30 l.min^{-1}). Furthermore, the eNGI has been used successfully to study the flow rate dependence of DPI aerosol performance and charge properties (Bricanyl™ and Pulmicort™ Turbuhalers) at 30, 60 and 90 l.min^{-1} (32).

To study the relationship between flow rate, electrostatic charge and aerosol performance, the authors report the use of the eNGI to simultaneously measure aerosol charge profiles and mass deposition in pMDI formulations at a series of flow rates: 30, 60 and 90 l.min^{-1}. In addition, the authors intend to investigate the contribution of individual components towards aerosol performance and charge properties of a combination pMDI formulation. Two commercially available products: Flixotide, (containing 250 μg FP) and Seretide (combination product containg 25 μg salmeterol xinafoate (SX) and 250 μg FP) were investigated for this study.

MATERIALS AND METHODS

Materials

Flixotide™ (250 μg.dose^{-1} fluticasone propionate (FP)) and Seretide™ (25 ug.dose^{-1} salmeterol xinafoate (SX) and 250 μg.dose^{-1} FP) (both Allen & Hanburys, Australia) were chosen as the model single and combination pMDI therapies, respectively. Both formulations contain a drug suspension in HFA-134a propellant with no further excipients included. Water (>2 MΩ cm resistivity at 25°C) was purified using a Modulab Type II Deionization System (Continental Water Systems, Sydney, Australia). Methanol and ammonium acetate were supplied by Sigma-Aldrich (St. Luis, USA). All compounds were of analytical grade and were used as received.

Aerosol and Electrostatic Characterisation Using the eNGI

The construction and specifications of the eNGI are described in more detail elsewhere (31,33). Simply, each eNGI collection cup is electrically isolated from the impactor housing. Upon assembly, each cup makes contact with a retractable BNC connector-UHF cable which, in-turn, is connected to one channel of a multi-channel femto-ampmeter (Keithley 6517A electrometer (with K521 10-channel scanner card); Keithley Instruments, USA). Upon operation, the multi-channel recorder reports the current on each stage to a connected personal computer for data recording and analysis.

Prior to measurements, the eNGI flow rate was set at either 30, 60 or 90 l.min^{-1} using a calibrated flow meter (TSI 3063, TSI instruments Ltd., Buckinghamshire, UK), Rotary vein pump and solenoid valve timer (Erweka GmbH, Germany). Each eNGI impactor plate was coated with silicone oil by submerging the plate in a 10% *v/v* silicone/hexane solution before placing in a fume-hood to air-dry for 10 min. After assembly of the eNGI, a USP stainless-steel throat (and mouthpiece adapter) were connected to the impactor and the current outputs zeroed for baseline at each flow rate (electrometer range 2 nA; scan speed = 10 channels.sec^{-1}). The operation of air flow at the aforementioned set values did not contribute to background charge.

The inhaler was primed once to waste as per manufacturer's instructions and four discrete actuations (7 s each) fired directly into the USP throat of the eNGI at one of the chosen flow rates. The pMDI was shaken thoroughly between each actuation and a 30 s delay instigated after the pump was switched on and after the pMDI was actuated. Current *vs.* time data from each stage was collected by the electrometer and recorded with Microsoft® Hyperterminal™ (Microsoft Corporation, USA). The data was integrated to produce plate charge data. After all four actuations were dispensed (equivalent to 100 μg SX and/or 1000 μg FP), the USP throat and collection cups were rinsed with diluent into appropriate volumetric flasks and assayed using high-performance liquid chromatography (HPLC). At each flow rate, three repeats for each pMDI formulation were conducted from a single inhaler. A new inhaler was used for every flow rate.

High-Performance Liquid Chromatography

Chemical analysis of FP and SX was performed by HPLC, based on a method described by Murnane *et al.*, (34). The system set up was as follows: LC20AT pump, SIL20AHT autosampler, CBM-Lite system controller with a PC-computer running LCsolution v1.22 software and an SPD-20A UV-VIS detector (Shimadzu, Sydney, NSW, Australia). A Hewlett-Packard Hypersil ODS 3 μm 150 mm×4.6 mm (Phenomenex, Sydney, Australia) was used for separation at a flow rate of 1 ml.min^{-1}. Mobile phase consisted of 75:25 %*v/v* methanol: aqueous ammonium acetate solution (0.6% *w/v*). Wash solution and sample diluent was 75:25 % *w/v* methanol:water. Standard solutions for FP and SX were prepared at concentrations of 200, 100, 50, 10, 1, and 0.1 μg.ml^{-1}. Quantitation was based on peak area, using a standard curve, which was prepared daily.

Statistical Analysis

Data were subjected to statistical analysis using the SPSS Statistics 17.0 software package (SPSS Inc, Chicago, Illinois, USA). Two Tailed students t-test and ANOVA one-way analysis (with Tukeys post hoc analysis) were utilised to test for significance. Significant difference was based on $p<0.05$.

RESULTS AND DISCUSSION

The deposition of both FP and SX in each stage of the eNGI was calculated as a percentage of the total sample recovery and represented as percent per stage/cut-off diameter. Cut-off diameters for each eNGI stage (Table I) were calculated from previously validated methodologies (29,30). The deposition patterns of FP in Flixotide™ (Fig. 1a) and Seretide™ (Fig. 1b) were similar in nature. Interestingly, an increase in flow from 60 l.min^{-1} to 90 l.min^{-1} resulted in a change in the upper stage deposition profile of FP, possibly due to increased turbulence, particle coalition and reduced throat and device deposition. Analysis of the SX stage deposition in the Seretide product (Fig. 1c) suggested high throat deposition with the majority of particles being deposited on stages 1 to 4 of the eNGI (corresponding to sizes between 1.3 and 6.4 μm; depending on flow rate).

A common method of representing aerosol performance is by classifying the mass or percentage of particles that have an aerodynamic diameter considered suitable for inhalation (typically ≤ 5 μm). The cumulative drug deposited on each

Table I. Cut-off Diameters for the eNGI at 30, 60 and 90 l.min^{-1} (diameters calculated from (29, 30))

Stage	30 l.min^{-1}	Stage	60 l.min^{-1}	Stage	90 l.min^{-1}
1	11.72 μm	1	8.06 μm	1	6.48 μm
2	6.4 μm	2	4.46 μm	2	3.61 μm
3	3.99 μm	3	2.82 μm	3	2.3 μm
4	2.3 μm	4	1.66 μm	4	1.37 μm
5	1.36 μm	5	0.94 μm	5	0.76 μm
6	0.83 μm	6	0.55 μm	6	0.43 μm
7	0.54 μm	7	0.34 μm	7	0.26 μm

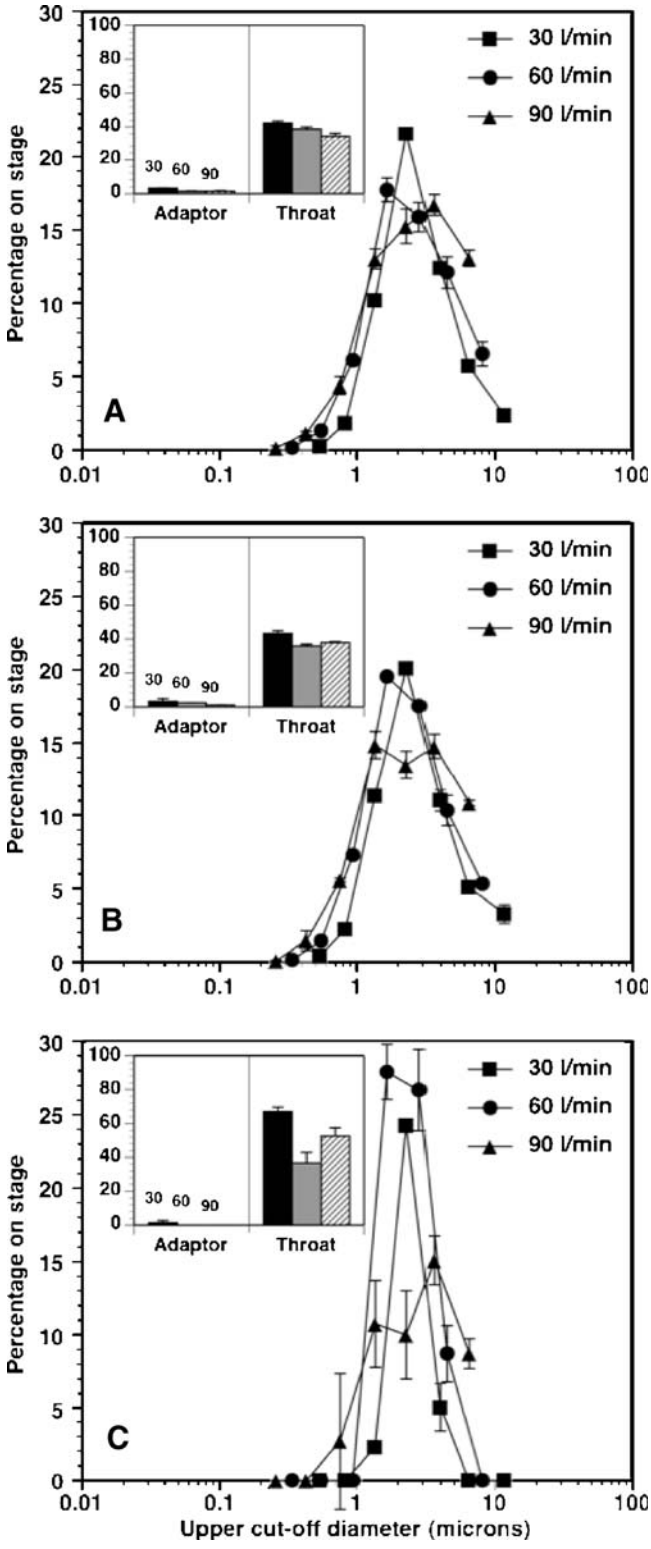

Fig. 1. Percentage deposition of fluticasone propionate (FP) or salmeterol (SX) across all stages of the eNGI; (A) FP in Flixotide™, (B) FP in Seretide™, (C) SX in Seretide™.

stage of the impactor was plotted as a function of the log-cut-off diameter (Table I) and linear regression was used to calculated the mass of drug < 5 μm (or fine particle dose, FPD). The FPD was calculated as a percentage of total emitted dose (ED) to give the fine particle fraction (FPF). ED and FPD values for fluticasone and salmeterol are presented in Table II.

Comparison of the FPF values of FP in both Flixotide™ and Seretide™ formulations indicated flow rate had a significant effect on the aerosolisation performance (ANOVA $p<0.05$) (Fig. 2). Post hoc analysis (Tukey's) indicated this to be significant between 30 $l.min^{-1}$ and 60 $l.min^{-1}$ for both products, where an increase in FPF from 35.39±0.52% to 41.50±1.25%, and 35.96±0.52% to 44.72±0.98%, was observed for Flixotide™ and Seretide™, respectively. The observed increase in FPF of Flixotide™ was in good agreement with previous studies by Feddah *et al.*, (who reported an FPF of 32.67%±2.1% at 30 $l.min^{-1}$, and 50.1%± 6.3% at 60 $l.min^{-1}$ (10)). To the authors' knowledge, no comparative data exists for Seretide™. A further increase in flow rate from 60 $l.min^{-1}$ to 90 $l.min^{-1}$ had no effect on the FPF of FP in either formulation. Comparison of the FPF of FP between products, at each flow rate indicated no significant difference. Such an observation is interesting, since the formulations are very different in nature (Seretide™ is a combination formulation containing also SX).

Comparison of the SX FPF in the Seretide™ product, as a function of flow rate, indicated that while an increase in the mean value was observed between 60 $l.min^{-1}$ and 90 $l.min^{-1}$, this was not significantly different (ANOVA $p<0.05$). No significant difference in FPF was seen between 30 $l.min^{-1}$ and 60 $l.min^{-1}$, as with the FP component of Seretide™. It is also interesting to note, that the SX FPF was generally lower than that for FP (the highest observed mean FPF for SX was 31.86%±0.77% at 90 $l.min^{-1}$). An atomic force microscopy (AFM) study of adhesion-cohesion forces by Young *et al.* (2004) indicated five-fold greater separation energy between SX and FP surfaces, compared to SX-SX and FP-FP interactions (35). Previous work by Michael *et al.* (2000, 2001) demonstrated that a mixed pMDI formulation of SX and FP features interaction between the two drugs, which results in the formation of hetero-flocs (36,37). Given that Seretide™ contains a small SX dose (25 μg) compared to that of FP (250 μg), it is possible that such interparticle interactions would have a greater impact on SX FPF than FP. For instance, 40–60% of SX is deposited in the USP throat, compared to 35–45% for FP.

The total drug mass deposition from Flixotide™ (FP) or Seretide™ (FP + SX) on each stage of the eNGI is shown in Fig. 3a and b, respectively. Total drug mass deposition is important since, partially, it will be directly related to the total charge capacity of the system. In general, the mass

Table II. Total Emitted Dose (ED) and Fine Particle Dose (FPD) of Fluticasone Propionate (FP) and Salmeterol (SX) from Flixotide™ and Seretide™ Relative to Flow Rate ($n=3$, mean ± SD)

		30 $l.min^{-1}$	60 $l.min^{-1}$	90 $l.min^{-1}$
FP (Flixotide)	FPD (μm)	90.5 (± 3.2)	112.5 (± 5.7)	125.5 (± 3.7)
	ED (μm)	255.5 (± 5.3)	271.1 (± 9.5)	291.4 (± 2.1)
FP (Seretide)	FPD (μm)	76.7 (± 1.6)	124.0 (± 8.7)	113.6 (± 1.0)
	ED (μm)	213.4 (± 5.9)	277.0 (± 13.7)	258.5 (± 6.2)
SX (Seretide)	FPD (μm)	6.5 (± 0.5)	7.0 (± 0.7)	7.1 (± 0.7)
	ED (μm)	24.1 (± 0.8)	26.0 (± 0.3)	22.4 (± 3.3)

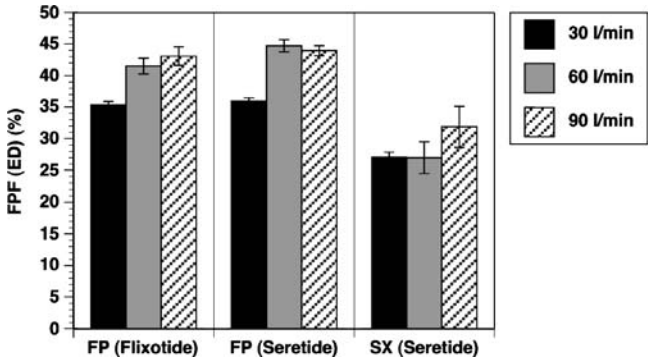

Fig. 2. Fine particle fraction of FP and SX from the Flixotide™ and Seretide™ product as a function of flow rate, (n=3).

depositions showed similar profiles to that of the percentage mass deposition shown in Fig. 1. As with the percentage component distributions (Fig. 1), an increase in flow rate from 30 l.min^{-1} to 60 lmin^{-1} results in a shift in particle distribution to lower cut-off diameters. Such observations are further substantiated by the significant difference in FPF of FP, between these two flow rates. Further increase from 60 l.min^{-1} to 90 lmin^{-1} results in a shift in the mass distribution profile, (specifically between ~1 μm and 10 μm); however, the variability profile is not observed in the FPF, since the sum of mass <5 μm does not change significantly.

Charge distributions of the Flixotide™ device, as a function of flow rate, are shown in Fig. 4a. The charge distribution of Flixotide™ at 30 l.min^{-1} was similar to previous reports using the ELPI (22,23) and eNGI (31). In general, the charge distribution followed a parabola shape with a negative charge distribution, mirroring the mass distribution observed on each stage. An increase in flow from 30 l.min^{-1} to 60 l.min^{-1} resulted in an increase in negative charge, primarily on the lower stages of the eNGI. This is most likely related to the increase in mass deposition on these stages rather than a significant increase in the specific charge associated with a particular size fraction. Further increase from 60 l.min^{-1} to 90 l.min^{-1} resulted in a change in the charge profile with the upper cut-off diameters having increased negative charge. This many be related to the paradigm shift in mass distribution profile for Flixotide at 90 l. min^{-1}; since an increased flow rate may induce a higher particle charge and subsequent interaction.

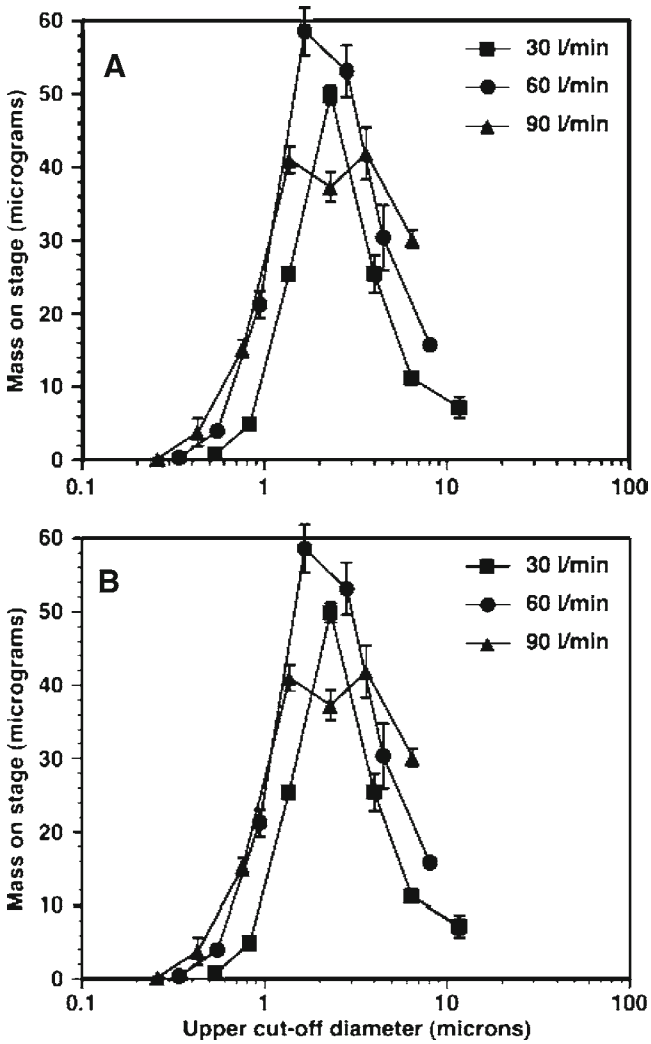

Fig. 3. Total drug mass deposition on each eNGI cascade impactor stages as a function of flow rate (A) Flixotide™ (FP), (B) Seretide™ (FP + SX), (n=3).

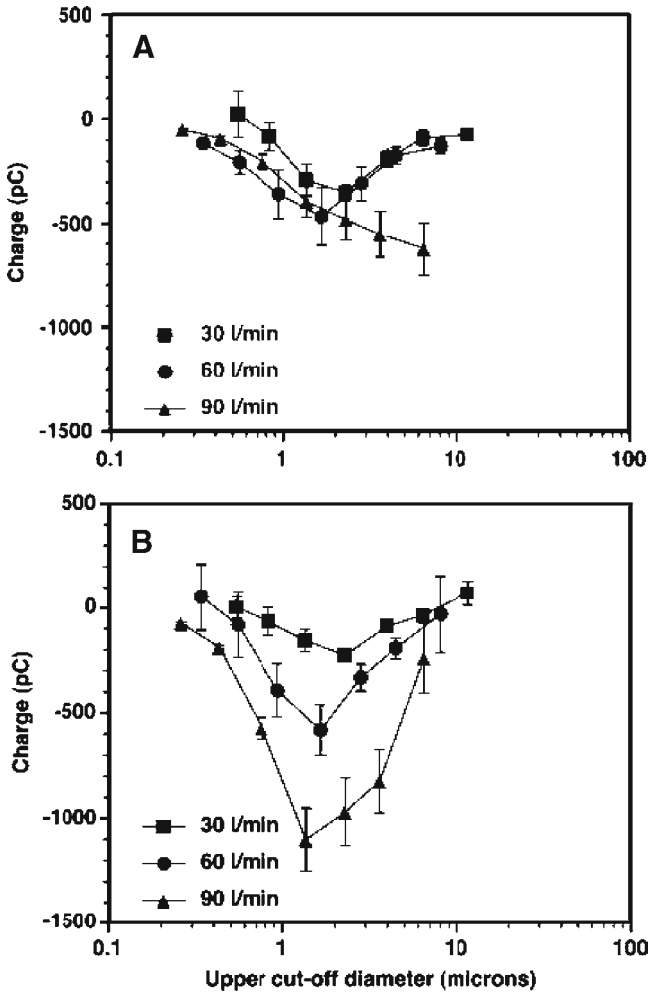

Fig. 4. Charge distribution as a function of eNGI stage and flow rate (A) Flixotide™ (B) Seretide™. (n=3).

Charge distributions of the combination Seretide™ pMDI formulation, as a function of flow rate, are shown in Fig. 4b. As with the Flixotide™ product, Seretide™ had a parabolic shaped negative charge distribution that mirrored the mass distribution profiles (Fig. 3b). In comparison to Flixotide™, increasing the flow rate from 30 l.min^{-1} to 60 l.min^{-1} (and subsequently to 90 l min^{-1}) resulted in a sequential increase in the negative charge profile. Furthermore, the higher flow rates for Seretide™ resulted in a greater negative charge even though the total mass distributions were similar to those of Flixotide™, at equivalent flow rates.

To further investigate the relationship between flow rate, particle size distribution and electrostatic charging, the charge data was divided by mass to produce charge-to-mass ratios (q/m) for each cut-off stage, thus creating a q/m distribution according to particle size. Charge to mass ratio data are useful since they allow quantitative analysis of the net charge carried on a specific size range; that is to say, q/m values eliminate the mass variation effects. The q/m distribution for Flixotide™ and Seretide™ are shown in Fig. 5a and b, respectively.

Analysis of the q/m values for Flixotide™ (excluding the lowest stage) suggested no significant difference between 30 l.min^{-1} and 60 l.min^{-1} flow rates. In comparison, an increase in flow rate from 60 l.min^{-1} to 90 l.min^{-1} resulted in a significant change in the q/m ratio, specifically at the higher cut-off diameters. Such observations correlate well with the change in aerosol mass and charge distribution over the same range. This indicates that there is an increase in larger particles (instigated via the increased flow rate) with a concurrent increase in number of electrons per-particle. Similarly, the q/m profile for Seretide™ changes as a function of flow rate. In general, an increase in flow rate from 30 l.min^{-1} to 90 l.min^{-1} results in a significant increase in the negative charge associated with the aerosol cloud. This negative deviation is more evident in lower cut-off diameters.

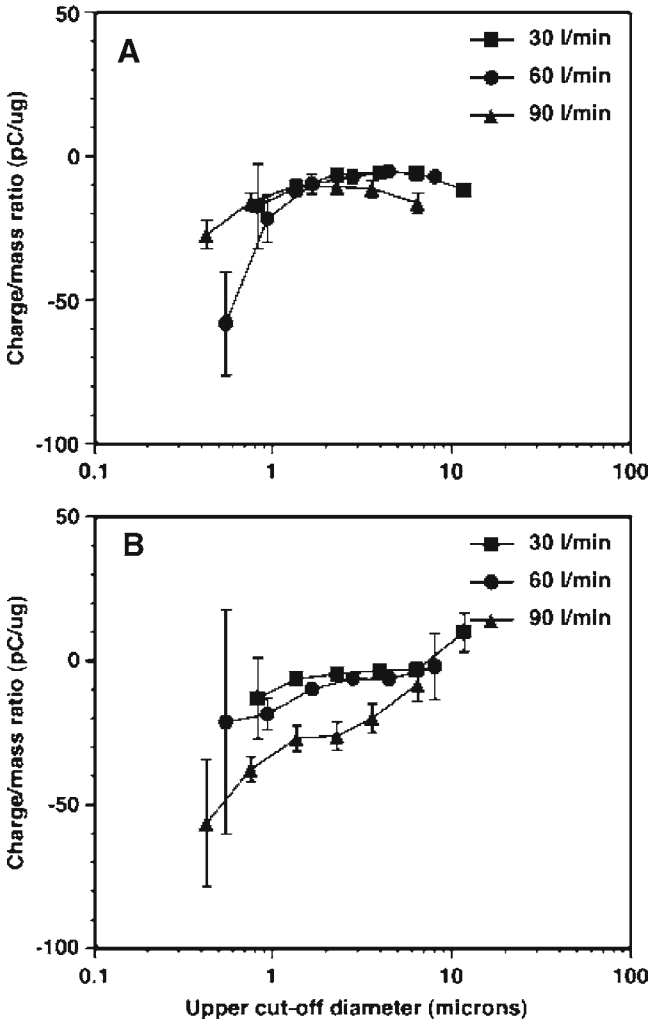

Fig. 5. Charge to mass ratio on each stage of the eNGI (A) Flixotide™ (B) Seretide™. (n=3).

Although the small aerodynamic diameter of fine particles assists their entrainment in the lower airways and alveoli, the charge carried by these particles may affect deposition. Bailey *et al.* (1997) and Balachandran *et al.* (1997) reported that, mathematically modelled fine particles with charge increased to 200 electrons/particle, may have its deposition in the lower airways enhanced by space and image charge forces, while a 5 μm particle carrying 3000 electrons/particle will have reduced lung deposition (12,38). However, it is difficult to apply these findings to the q/m results in this study since it refers to size fractions, not individual particles. In addition, these models do not include a scenario where there are multiple fine components, as is the case with Seretide. As an example, estimates of Seretide elemental charge for the size fractions 2.3–3.99 μm (30 l.min^{-1}), 28.2–4.46 μm (60 l.min^{-1}), and 2.3–3.61 μm (90 l.min^{-1}) give −5500, −12000 and −27000, respectively. Nevertheless, from 30 to 60 l.min^{-1}, FPD, ED and FPF increase, while there is no significant difference in Seretide FPF from 60 to 90 l.min^{-1} (Fig. 2). As such, it is still unclear as to whether electrostatic charge has any significant effect on pMDI drug deposition during inhalation, as claimed by the studies quoted above, as well as previous *in vitro* studies (14,15). An interesting observation is that the q/m standard deviations for the lowest impactor stages are large. Since the lower stages contain very small mass values, the charge to mass division results in large and variable q/m values. However, even taking these errors into account, the q/m values are very high, likely due to the high specific surface area available for contact charging during collisions with larger particles and the inhaler.

It is difficult to speculate the reasons for the differences in q/m with flow rate and formulation, since reviewing electrostatic and triboelectrification phenomena in insulating materials literature, shows that this area is not fully developed. However, from this study, it is evident that at higher flow rates the aerosol particles carry a greater charge, and there is a difference in charge profiles between a fluticasone-only and fluticasone-salmeterol formulation. Electron transfer between materials with a high work function to material with low work function is likely to be the mechanism by which particle charging occurs. Despite appearing to be simple in design, pMDIs contain multiple materials (including the canister, valve stem, actuator block, HFA, and drug). Although both Flixotide™ and Seretide™ charge profiles are unipolar negative, within each size fraction may contain bipolarly charged particles which produce a net negative charge as a whole. Sources of bipolar charging can include charge separation during deaggregation, contact between fluticasone and salmeterol particles, contact between coarse

and fine particles (39,40) or contact with the inhaler surface. Speculation of this dynamic charging mechanism is difficult, since each component cannot be studied in isolation. Subsequently, it is suggested a systematic study of these components be studied in isolation in future, from a model system rather than a marked product.

CONCLUSION

This study has demonstrated how the eNGI is capable of investigating the mass and charge distributions of both single and combination pMDI formulations at flow rates relative to patient inhalation. Significant differences in the mass distributions and charge profiles of both Flixotide™ and Seretide™ were observed. While, the reason for such observations are speculative, and require a fundamental investigation (in terms of surface chemistry and the mechanism of charging), this study highlights the importance of such factors and may have direct implications on therapeutic properties of pMDI formulations.

REFERENCES

1. Pritchard JN. The influence of lung deposition on clinical response 1. J Aerosol Med. 2001;14:S19–26.
2. Bennett WD, Brown JS, Zeman KL, Hu SC, Scheuch G, Sommerer K. Targeting delivery of aerosols to different lung regions. J Aerosol Med. 2002;15(2):179–88.
3. Chapter < 601 > (2008),. United States Pharmacopeia 31—National Formulary 26, : United States Pharmacopeial Convention Inc.; 2008.
4. Section 2.9.18—appendix XII C. Consistency of Formulated Preparations for inhalation. British Pharmacopoeia 2009.
5. Ross DL, Schultz RK. Effect of inhalation flow rate on the dosing characteristics of dry powder inhaler (DPI) and metered dose inhaler (MDI) products. J Aerosol Med. 1996;9(2):215–26.
6. Terzano C, Mannino F. Aerosol characterization of three corticosteroid metered dose inhalers with volumatic holding chambers and metered dose inhalers alone at two inspiratory flow rates. J Aerosol Med. 1999;12(4):249–54.
7. Mitchell JP, Nagel MW. Time-of-flight aerodynamic particle size analyzers: their use and limitations for the evaluation of medical aerosols. J Aerosol Med. 1999;12(4):217–40.
8. Mitchell JP, Nagel MW, Cheng YS. Use of the aerosizer (R) aerodynamic particle size analyzer to characterize aerosols from pressurized metered-dose inhalers (pMDIs) for medication delivery. J Aerosol Sci. 1999;30(4):467–77.
9. Smith KJ, Chan HK, Brown KF. Influence of flow rate on aerosol particle size distributions from pressurized and breath-actuated inhalers. J Aerosol Med. 1998;11(4):231–45.
10. Feddah MR, Brown KF, Gipps EM, Davies NM. *In-vitro* characterisation of metered dose inhaler *versus* dry powder inhaler glucocorticoid products: influence of inspiratory flow rates. J Pharm Pharm Sci. 2000;3(3):318–24.
11. Bailey AG. The inhalation and deposition of charged particles within the human lung. J Electrostat. 1997;42(1–2):25–32.
12. Balachandran W, Machowski W, Gaura E, Hudson C. Control of drug aerosol in human airways using electrostatic forces. J Electrostat. 1997;40–1:579–84.
13. Koolpiruck D, Prakoonwit S, Balachandran W. Numerical modeling of inhaled charged aerosol deposition in human airways. Ieee T Ind Appl. 2004;40(5):1239–48.
14. Ali M, Mazumder MK, Martonen TB. Measurements of electrodynamic effects on the deposition of MDI and DPI aerosols in a replica cast of human oral-pharyngeal-laryngeal airways. J Aerosol Med Pulm D. 2009;22(1):35–44.
15. Ali M, Reddy RN, Mazumder MK. Electrostatic charge effect on respirable aerosol particle deposition in a cadaver based throat cast replica. J Electrostat [Article]. 2008;66(7–8):401–6.
16. Melandri C, Tarroni G, Prodi V, Dezaiacomo T, Formignani M, Lombardi CC. Deposition of charged-particles in the human airways. J Aerosol Sci. 1983;14(5):657–69.
17. Kwok PCL, Collins R, Chan HK. Effect of spacers on the electrostatic charge properties of metered dose inhaler aerosols. J Aerosol Sci. 2006;37(12):1671–82.
18. Lipworth BJ, Lee DKC, Anhoj J, Bisgaard H. Effect of plastic spacer handling on salbutamol lung deposition in asthmatic children. Brit J Clin Pharmaco. 2002;54(5):544–7.
19. Mitchell JP, Coppolo DP, Nagel MW. Electrostatics and inhaled medications: influence on delivery via pressurized metered-dose inhalers and add-on devices. Respir Care. 2007;52(3):283–300.
20. Newman SP. Spacer devices for metered dose inhalers. Clin Pharmacokinet. 2004;43(6):349–60.
21. Keskinen J, Pietarinen K, Lehtimaki M. Electrical low-pressure impactor. J Aerosol Sci. 1992;23(4):353–60.
22. Glover W, Chan HK. Electrostatic charge characterization of pharmaceutical aerosols using electrical low-pressure impaction (ELPI). J Aerosol Sci. 2004;35(6):755–64.
23. Kwok PCL, Glover W, Chan HK. Electrostatic charge characteristics of aerosols produced from metered dose inhalers. J Pharm Sci-Us. 2005;94(12):2789–99.
24. Kotian R, Peart J, Bryner J, Byron PR. Calibration of the modified electrical low-pressure impactor (ELPI) for use with pressurized pharmaceutical aerosols. J Aerosol Med Pulm D. 2009;22(1):55–65.
25. Electrical Low Pressure Impactor product specifications. Osuusmyllynkatu 13, FIN-33700 Tampere, Finland : Dekati Ltd.; 2009.
26. Saini D, Biris AS, Srirama PK, Mazumder MK. Particle size and charge distribution analysis of pharmaceutical aerosols generated by inhalers. Pharm Dev Technol. 2007;12(1):35–41.
27. Philip VA, Mehta RC, Mazumder MK, DeLuca PP. Effect of surface treatment on the respirable fractions of PLGA microspheres formulated for dry powder inhalers. Int J Pharm. 1997;151(2):165–74.
28. Yurteri CU, Mazumder MK, Grable N, Ahuja G, Trigwell S, Biris AS, *et al.* Electrostatic effects on dispersion, transport, and deposition of fine pharmaceutical powders: development of an experimental method for quantitative analysis. Part Sci Technol. 2002;20(1):59–79.
29. Marple VA, Olson BA, Santhanakrishnan K, Mitchell JP, Murray SC, Hudson-Curtis BL. Next generation pharmaceutical impactor (a new impactor for pharmaceutical inhaler testing). Part II: Archival calibration. J Aerosol Med. 2003;16(3):301–24.
30. Marple VA, Roberts DL, Romay FJ, Miller NC, Truman KG, Van Oort M, *et al.* Next generation pharmaceutical impactor (a new impactor for pharmaceutical inhaler testing). Part I: Design. J Aerosol Med. 2003;16(3):283–99.
31. Hoe S, Young PM, Chan HK, Traini D. Introduction of the electrical next generation impactor (eNGI) and investigation of its capabilities for the study of pressurized metered dose inhalers. Pharm Res. 2009;26(2):431–7.
32. Hoe S, Traini D, Chan H-K, Young PM. Measuring charge and mass distributions in dry powder inhalers using the electrical Next Generation Impactor (eNGI). Eur J Pharm Sci. 2009;38(2):88–94.
33. Hoe S, Traini D, Chan HK, Young PM. The electrical next generation impactor. Inhalation. 2009:*in press*.
34. Murnane D, Martin GP, Marriott C. Validation of a reverse-phase high performance liquid chromatographic method for concurrent assay of a weak base (salmeterol xinafoate) and a pharmacologically active steroid (fluticasone propionate). J Pharm Biomed Anal. 2006;40(5):1149–54.
35. Young PM, Price R, Jones S, Billings M-P. Investigation into drug and excipient interaction in dry powder inhaler combination products. In: Dalby RN, Byron PR, Peart J, Suman JD, Farr SJ, editors. Respiratory drug delivery IX; California. USA: Davis Healthcare International Publishing; 2004. p. 749–51.
36. Michael Y, Chowdhry BZ, Ashurst IC, Snowden MJ, Davies-Cutting C, Gray S. The physico-chemical properties of salmeterol and fluticasone propionate in different solvent environments. Int J Pharm. 2000;200(2):279–88.

37. Michael Y, Snowden MJ, Chowdhry BZ, Ashurst IC, Davies-Cutting CJ, Riley T. Characterisation of the aggregation behaviour in a salmeterol and fluticasone propionate inhalation aerosol system. Int J Pharm. 2001;221(1–2):165–74.
38. Bailey AG, Hashish AH, Williams TJ. Drug delivery by inhalation of charged particles. J Electrostat. 1997;44(1–2):3–10.
39. Ali FS, Ali MA, Ali RA. Inculet, II. Minority charge separation in falling particles with bipolar charge. J Electrostat. 1998;45 (2):139–55.
40. Lacks DJ, Levandovsky A. Effect of particle size distribution on the polarity of triboelectric charging in granular insulator systems. J Electrostat. 2007;65(2):107–12.